In Utero Exposure to Second-Hand Smoke Aggravates Adult Responses to Irritants

Adult Second-Hand Smoke

Rui Xiao[1], Zakia Perveen[1], Daniel Paulsen[2], Rodney Rouse[3], Namasivayam Ambalavanan[4], Michael Kearney[2], and Arthur L. Penn[1]

[1]Department of Comparative Biomedical Sciences, and [2]Department of Pathobiological Sciences, School of Veterinary Medicine, Louisiana State University, Baton Rouge, Louisiana; [3]United States Food Drug Administration, Silver Spring, Maryland; and [4]Department of Pediatrics, University of Alabama at Birmingham, Birmingham, Alabama

***In utero* exposure to second-hand smoke (SHS) is associated with exacerbated asthmatic responses in children. We tested the hypothesis that *in utero* SHS will aggravate the lung responses of young adult mice re-exposed to SHS. We exposed Balb/c mice *in utero* to SHS (S) or filtered air (AIR; A), and re-exposed the male offspring daily from 11–15 weeks of age to either SHS (AS and SS) or AIR (AA and SA). After the adult exposures, we analyzed samples of bronchoalveolar lavage fluid (BALF), examined the results of histopathology, and assessed pulmonary function and gene expression changes in lung samples. In SS mice, compared with the other three groups (AA, AS, and SA), we found decreases in breathing frequency and increases in airway hyperresponsiveness (AHR), as well as low but significantly elevated concentrations of BALF proinflammatory cytokines (IL-1b, IL-6, and keratinocyte-derived chemokine). Lung morphometric analyses revealed enlarged airspaces and arteries in SA and SS mice compared with their *in utero* AIR counterparts, as well as increased collagen deposition in AS and SS mice. Unique gene expression profiles were found for *in utero*, adult, and combined exposures, as well as for mice with elevated AHR responses. The profibrotic metalloprotease genes, *Adamts9* and *Mmp3*, were up-regulated in the SS and AHR groups, suggesting a role for *in utero* SHS exposure on the adult development of chronic obstructive pulmonary disease. Our results indicate that *in utero* exposures to environmentally relevant concentrations of SHS alter lung structure more severely than do adult SHS exposures of longer duration. These *in utero* exposures also aggravate AHR and promote a profibrotic milieu in adult lungs.**

Keywords: second-hand smoke; *in utero* exposure; airway hyperresponsiveness; lung structure changes; gene expression

CLINICAL RELEVANCE

We examined the lung responses of male BALB/c mice exposed *in utero* and then as adults to second-hand smoke (SHS). Our results indicate that *in utero* exposures to environmentally relevant concentrations of SHS (*1*) alter lung structure more severely than do adult SHS exposures of longer duration; (*2*) aggravate airway hyperresponsiveness; and (*3*) promote a profibrotic milieu in adult lungs.

In utero exposure to second-hand smoke (SHS), which exerts striking effects on lung function (1), has been associated with exacerbated asthmatic responses in children (1, 2). Altered lung function, an increased risk of asthma, and persistent lung function deficits in children have been linked with *in utero* and postnatal exposures to SHS (3–7). The synergistic effects of *in utero* smoke exposure with various nontobacco allergens have also been reported. Mild *in utero* SHS exposure exacerbates responses of BALB/c mice exposed to ovalbumin (OVA) from 11–15 weeks of age (8). These functional, histological, and inflammatory responses are accompanied by distinct changes in lung gene expression (9). Children exposed *in utero* to maternal smoking manifest a higher risk of sensitization to house dust mites (10). A recent study of mice found that *in utero* smoke exposure promotes Th2 polarization and induces allergic asthma in response to *Aspergillus fumigatus* sensitization (11). Whether and how *in utero* SHS exposures potentiate subsequent adult physiological and transcriptome responses to SHS exposure, without any other irritant challenges, are not fully understood.

Evidence also indicates that exposure to environmental pollutants, such as SHS, during crucial periods of prenatal and postnatal development alters the course of lung morphogenesis and maturation, potentially resulting in long-term changes that affect the function and structure of the respiratory system (12). Persistent adult SHS exposure is strongly associated with the development of chronic obstructive pulmonary disease (COPD), accounting for more than 80% of COPD cases in the United States (13). The effects of relatively brief SHS exposures *in utero* on the lung structure and pathogenesis of COPD have received little attention.

In the experiments described here, we tested the hypothesis that *in utero* exposure to SHS will aggravate lung responses of young adult mice re-exposed to SHS. We asked whether *in utero* and adult exposures to SHS exert significant effects on murine lungs with regard to:

- Lung inflammation and proinflammatory cytokine production;
- Lung morphology (airway and vasculature);
- Lung function, including airway hyperresponsiveness (AHR) and breathing patterns; and
- Gene expression patterns.

We focused particularly on whether mice exposed *in utero* or as adults to SHS respond differently from each other and from mice exposed to SHS both *in utero* and as adults.

MATERIALS AND METHODS

Animal Protocols

We housed and handled BALB/c mice (Harlan, Indianapolis, IN) as described previously (8). The Institutional Animal Care and Use Committee

(*Received in original form July 5, 2012 and in final form August 17, 2012*)

This work was supported by the Louisiana Governor's Biotechnology Initiative (A.L.P.) and by National Institutes of Health grant HL092906 (N.A.).

Correspondence and requests for reprints should be addressed to Arthur L. Penn, Ph.D., Department of Comparative Biomedical Sciences, School of Veterinary Medicine, Louisiana State University, Skip Bertman Drive, Room 2425, Baton Rouge, LA 70803. E-mail: apenn@vetmed.lsu.edu

This article has an online supplement, which is accessible from this issue's table of contents at www.atsjournals.org

Am J Respir Cell Mol Biol Vol 47, Iss. 6, pp 843–851, Dec 2012
Published 2012 by the American Thoracic Society
Originally Published in Press as DOI: 10.1165/rcmb.2012-0241OC on September 6, 2012
Internet address: www.atsjournals.org

at Louisiana State University approved all animal procedures. Pregnant mice were housed in separate cages from Day 20 of pregnancy until weaning (Postnatal Day 21).

SHS Exposures

Sidestream smoke, which comprises 85–90% of SHS, served as a surrogate for SHS (14, 15). Smoke exposures and related measurements were performed as previously described (8), except that 3R4F filtered research cigarettes (University of Kentucky, Lexington, KY) were used to achieve a suspended particle density of 10 mg/m^3. The 3R4F cigarette is a model of a "full flavor" (10 mg tar), commercially available, filtered cigarette (16). Investigations performed with an earlier version of this model cigarette (1R4F) revealed that the inhalation-chamber SHS concentration produced by the steady-state combustion of one 1R4F cigarette was exceeded by the SHS concentration in bars where five smokers were seated at a table (17). In the experiment reported here, pregnant mice, and subsequently their male offspring, were exposed in inhalation chambers to a steady-state suspended particle concentration of 10 mg/m^3 and an average carbon monoxide concentration of 45 parts per million, concentrations 4–10 times higher than those generated in the earlier one-cigarette steady-state study.

After 5 days of mating, 10-week-old female mice were exposed to SHS mixed with high-efficiency particulate air–filtered air (AIR) or AIR alone (14 air changes/hour, 5 hours/day, for 19 consecutive days) in 1.3-m^3 stainless steel and Plexiglas dynamic exposure chambers. Male offspring were re-exposed to SHS or AIR from 11–15 weeks of age. Insufficient numbers of female mice were produced by these matings to allow for equivalent size groups of females to be tested. The exposure schedule is presented in Figure 1. Mice were classified into one of four groups, depending on whether SHS (S) or AIR (A) exposures were performed *in utero* or in adults (AA, $n = 7$; AS, $n = 8$; SA, $n = 6$; SS, $n = 6$). Colors representing the four exposure groups used consistently in Figures 2–4 and 6B (AA = orange; AS = green; SA = blue; SS = purple).

Pulmonary Function Testing

Pulmonary function testing was performed as previously described (8). In these pulmonary function studies, for each mouse at each methacholine dose concentration, readings over 5 minutes were averaged. Enhanced pause (Penh) values represent the degree of AHR in each animal. These data were used to generate the graph in Figure 4A. The highest Penh value (MaxPenh) recorded for each mouse sampled in the microarray study, regardless of methacholine dose (Figure 6B), is presented along with the array results for that mouse. A similar approach was used to calculate minimum breathing frequency (Figure 6A).

Cytokine Quantitation in BALF

Murine proinflammatory cytokine 7-plex kits (Meso Scale Discovery, Gaithersburg, MD) were used to measure major proinflammatory cytokines in BALF. The cytokines in the assay included IL-1b, IL-12p70, IFN-γ, IL-6, keratinocyte-derived chemokine (KC)/GRO, IL-10, and TNF-α. The manufacturer's stated average limits of detection (based on multiple kit lots) were 0.75, 35, 0.38, 4.5, 3.3, 11, and 0.85 pg/ml, respectively.

Histopathologic Analysis of Lungs

After BALF collection, lungs were fixed and processed as previously described (8, 14). We used a six-category scoring system (peribronchial, perivascular, bronchitis, pleuritis, alveolitis, and mucous metaplasia) for the evaluation of lung inflammation. Sites were scored from 0 (none) to 4 (severe). A board-certified veterinary pathologist, blinded to the treatments, evaluated histopathologic samples. A higher score (maximum score, 24) indicates greater tissue inflammation.

Lung Morphometric Analysis

The mean linear intercept (MLI) was measured in six ×100 random fields/slide. The radial alveolar count (RAC) was measured in six ×100 fields, each of which had a bronchiole termination that could be followed out to the pleura. Each value (MLI or RAC) represents the average of the six fields from each slide (animal) (18). Some RAC measurements involved fewer than six fields, because we could only identify four bronchi in those sections that could be followed out. For vascular morphometry, 20 random arteries accompanying airways were evaluated. Capillaries (< 20 μm) or large arteries (> 150 μm) were not evaluated. Wall thickness was calculated using the formula ($2 \times$ [WT/ED] $\times$ 100%), where WT = wall thickness, and ED = external diameter. We used a Nikon (Melville, NY) TE2000 microscope equipped with a QImaging (Surrey, BC, Canada) cooled high-resolution CCD camera and Metamorph image analysis software (version 6.2r4) for measurements (Molecular Devices, Sunnyvale, CA).

Statistical Analysis

We used the SAS statistical package (version 9.1.3; SAS Institute, Inc., Cary, NC) for data analyses. We performed one-way ANOVA on plethysmograph results, performed a Kruskal-Wallis test (one-way ANOVA) on the ranks for the cytokine data in considering limits of detection, and a *t* test for pairwise comparisons between two combined groups for morphometric analyses. When significant differences were found in the ANOVA model, we performed *post hoc* pairwise comparisons with the Tukey honest significant difference test. In all cases, we considered comparisons significant at $P < 0.05$. All error bars indicate means ± SDs.

Lung Harvest and mRNA Extraction

We followed previously described procedures (8). We checked the quantity and purity of RNA samples with a NanoDrop ND-1000 Spectrophotometer (NanoDrop, Wilmington, DE). Values generated from the NanoDrop for all samples fell into the following ranges: 260/280 ratio, 2.13–2.43; 260/230 ratio, 1.95–2.34; concentration, 622–1283 ng/μl. We performed further quality assays on 1:5 dilutions of RNA samples with an Agilent 2100 BioAnalyzer and Agilent RNA 6000 Nano Series II Kits (Agilent Technologies, Palo Alto, CA). All samples fell into the following ranges: 28S/18S ratio, 1.4–1.6; RNA integrity number, 8.9–9.6.

Microarray Assay

We assessed global gene expression in the lungs of individual 15-week-old mice (four male mice per treatment group) on murine 430.2 genome arrays (Affymetrix, Santa Clara, CA) representing more than 39,000 transcripts with more than 45,000 probe sets. Arrays were processed at

In-Utero Exposure	Adult Exposure	Symbol	# male offspring
Air	Air	AA	7
Air	SHS	AS	8
SHS	Air	SA	6
SHS	SHS	SS	6

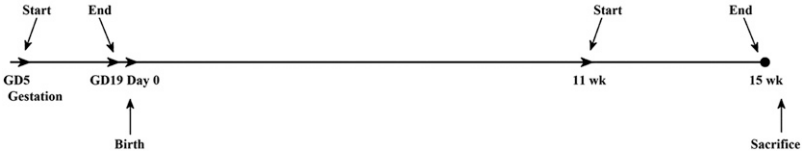

Figure 1. Group designations and experimental timeline. The two-letter symbols are assigned to four experimental groups, depending on their exposure status at both time points. Times shown in the experimental timeline are expressed relative to the birth date of offspring. AA, exposure to air *in utero* and as adults; AS, exposure to air *in utero* and to smoke as adults; GD, gestational day; SA, exposure to smoke *in utero* and to air as adults; SHS, second-hand smoke; SS, exposure to smoke *in utero* and as adults; wk, weeks.

the Research Core Facility of the Louisiana State University Health Science Center at Shreveport, as described previously (8).

Gene Expression Profiling

All analyses were performed in the R/bioconductor platform (http://www.r-project.org/; http://www.bioconductor.org/). All 16 arrays were preprocessed according to the robust multiarray average method to generate comparable expression values across all samples. A linear model for 2 × 2 factorial design ([*In Utero* Exposure] * [Adult Exposure]) was constructed with the Limma package (19) to select those genes that are highly associated with *in utero* or adult exposures. Associations between gene expression and phenotypic variables were tested in phenoTest (20). Correlation graphs and heat maps were plotted using the gclus and Heatplus (21) packages. We adopted a red–yellow color scheme to visualize the relative expression differences across all samples (Figures 5 and 6B), with red (negative row z-scores) indicating relatively low expression, and yellow (positive row z-scores) indicating relatively high expression. We used a green–red color scheme to indicate fold-change differences for pairwise comparisons, (Figure 7C). The microarray data have been deposited in the National Center for Biotechnology Information Gene Expression Omnibus (GEO; http://www.ncbi.nlm.nih.gov/geo/), and are accessible through GEO Series accession number GSE36810.

Gene-Set Functional Analysis and Ingenuity Pathway Analysis

Gene lists generated from statistical analyses were analyzed in the Web-Based Gene Set Analysis Toolkit (WebGestalt2) (22). Degrees of enrichment were calculated based on the gene lists with assistance from different public databases, including Gene Ontology (GO), Kyoto Encyclopedia of Genes and Genomes (KEGG), and Molecular Signatures Data Base (MSigDB). We analyzed gene expression data with Ingenuity Pathways Analysis (IPA) version 8.7 (Ingenuity Systems, Redwood City, CA). Gene networks and canonical pathways were examined using the Ingenuity Analysis Knowledge Database (Ingenuity Systems). We created custom gene networks to demonstrate the connections between the genes and significantly associated functional and signaling pathways identified in this study.

Quantitative RT-PCR

Total RNA was reverse-transcribed with a High Capacity cDNA reverse transcription kit (Applied Biosystems, Foster City, CA). Expression levels of selected genes were measured with a TaqMan universal PCR master mix (Applied Biosystems) and predesigned Taqman probes for murine genes (assay identifications: Hprt1, Mm00446968_m1; Gata3, Mm00484683_m1; Cyp1a1, Mm00487218_m1; Adamts9, Mm00614433_m1; Fam107a, Mm01706977_s1; Egr1, Mm00656724_m1; Fos, Mm00487425_m1; Btg2, Mm00476162_m1; Zfp36, Mm00457144_m1; and Nr4a1, Mm01300401_m1). Expression levels were normalized to Hprt1 concentrations.

RESULTS

Neutrophil concentrations in cell differentials were very low in all four groups, and were indistinguishable from each other (data not presented). We detected no evidence of lung inflammation.

Concentrations of the BALF cytokines IL-1b, IL-6, and KC were low, but were significantly increased (Tukey honest significant difference test, $P < 0.05$) in the SS group compared with the other three groups (Figure 2). IL-10, IL-12p70, TNF-α, and IFN-γ were not detected in any samples.

Lung morphometric analyses assessed MLIs, RACs, and vascular morphometric parameters, including artery wall thickness (WT), artery external diameter (ED), and percentage of wall thickness (% WT; Figure 3A). We found no statistically significant differences when results for the four individual groups were compared, although we detected indications of *in utero* exposure–related responses. After regrouping the four groups into two groups according to their *in utero* exposure status, significant increases were evident in MLIs, WT, and EDs in SX versus AX mice (SX = SA and SS combined, $n = 12$; AX = AA and AS combined, $n = 15$; Tukey honest significant difference test, $P < 0.05$). Evidence of increased perivascular collagen deposition was detected in the AS and SS groups (Figure 3B).

Pulmonary function testing revealed significantly elevated AHR in the SS group after methacholine challenge, compared with *in utero* (SA) or adult (AS) SHS exposure alone (Figure 4A). A reverse trend was found for breathing frequency (Figure 4B). Significant differences (Tukey honest significant difference test, $P < 0.05$) were found in enhanced pause (Penh) and breathing frequency (f) between the SS group and the other three groups at the highest methacholine dose (50 mg/ml). At methacholine doses ⩽ 12 mg/ml, both the AS and SS groups exhibited higher responses than did the SA and AA groups (both exposed to AIR as adults), whereas further increases in methacholine dose differentiated the SS group from each of the other three groups.

Gene expression profiling via a linear model revealed three sets of genes that were uniquely affected by *in utero* SHS exposure ($n = 232$), adult SHS exposure ($n = 5{,}547$), or both *in utero* and adult SHS exposure ($n = 183$), as shown by the Venn diagram in Figure 5. All genes in each group exhibited P values and false discovery rate (FDR) values < 0.05. Adult exposure to SHS yielded 20 times

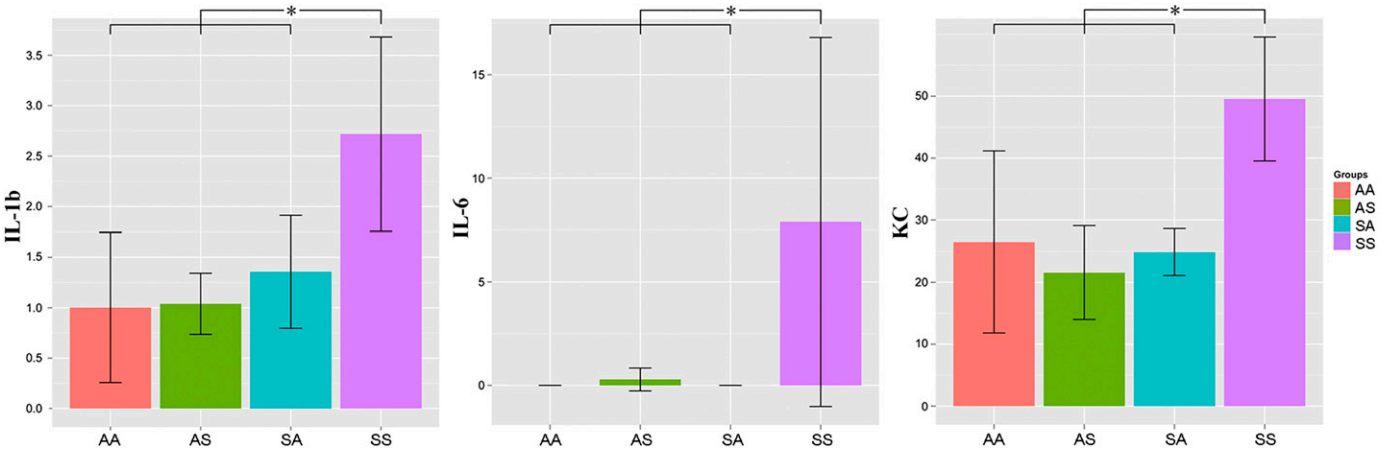

Figure 2. Mice in the SS group expressed significantly higher concentrations of the cytokines IL-1b, IL-6, and keratinocyte-derived chemokine (KC), compared with mice in the other three groups (ANOVA on ranks, $P < 0.05$, *post hoc* Holm-Sidak test). IL-10, IL-12p70, and IFN-γ were not detectable in any group. Each bar represents the mean ± SD.

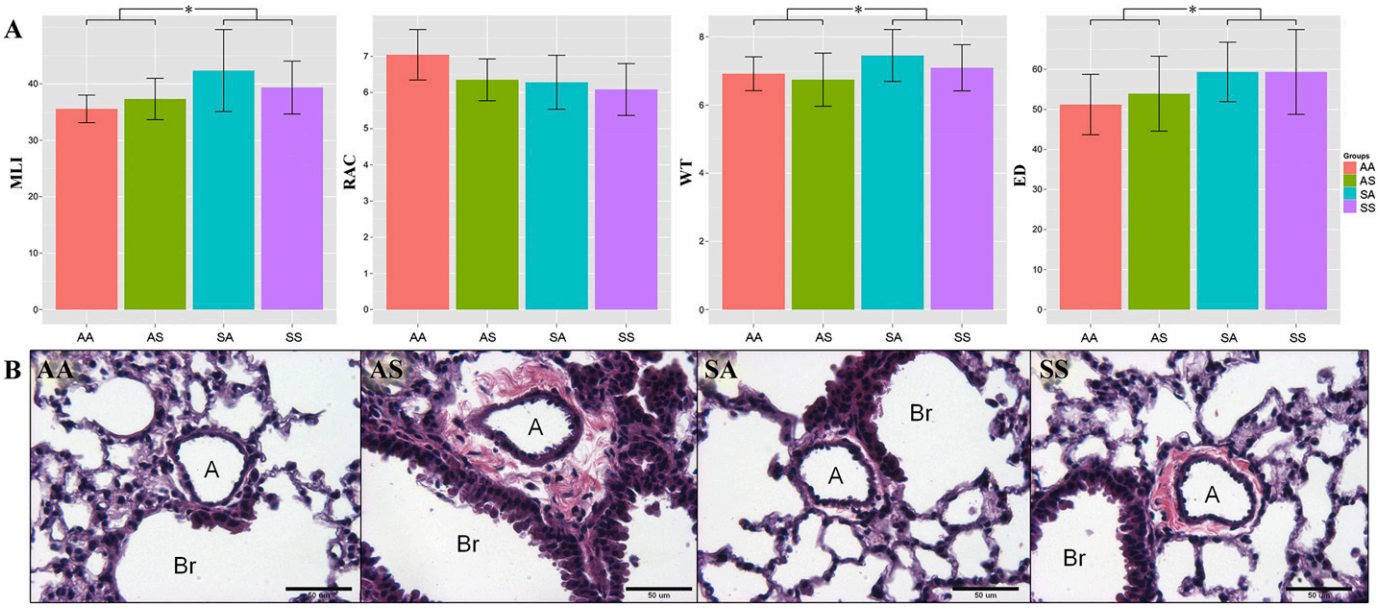

Figure 3. (*A*) *In utero* but not adult exposure significantly affected lung morphometric results (increased MLI, and increased arterial WT and ED) in 15-week-old male mice. Each bar represents the mean ± SD. (*B*) Representative slides showed increased collagen deposition around the arteries in the AS and SS groups. A, artery; Br, bronchiole; ED, external diameter; MLI, mean linear intercept; RAC, radial alveolar count; WT, wall thickness.

more differentially expressed genes than did *in utero* SHS exposure. Relatively low (Figure 5, *red*) or high (Figure 5, *yellow*) expression levels across all samples were plotted in heat maps and confirmed that in each case, the gene expression patterns were dependent on the timing of SHS exposure.

The correlation scatterplot (Figure 6A) revealed that cytokine concentrations correlated well with physiological measurements. The measurement with the highest correlation was of MaxPenh ($r_{(\text{IL-1b, MaxPenh})} = 0.66$, $r_{(\text{IL-6, MaxPenh})} = 0.83$). Therefore, we selected MaxPenh to represent AHR, and correlated this set of readings with each gene on the microarray. We found 323 probes, each with P value and FDR < 0.05. All 323 probes were plotted in a heat map, with MaxPenh values also shown below the heat map (Figure 6B).

For each of the four gene lists (*in utero* only, adult only, and *in utero* + adult, Figure 5; AHR, Figure 6B), the 10 most up-regulated/down-regulated genes (SS versus AA, i.e., doubly exposed to SHS versus never exposed) in each list are presented in Figure 7A. The differential expression of several genes initially identified by microarray analysis, and highlighted in Figure 7A, was further confirmed by quantitative RT-PCR. The quantitative RT-PCR results (Figure 7B) yielded comparable fold-change values (numbers shown for each gene) between SS (Figure 7, *purple*) and AA (Figure 7, *blue*). Thus, the quantitative RT-PCR results confirm the microarray-based findings. The ΔΔCT values (for the gene of interest compared with the housekeeping gene, Hprt1) are charted in Figure 7B. For each comparison, the Hprt1 value is

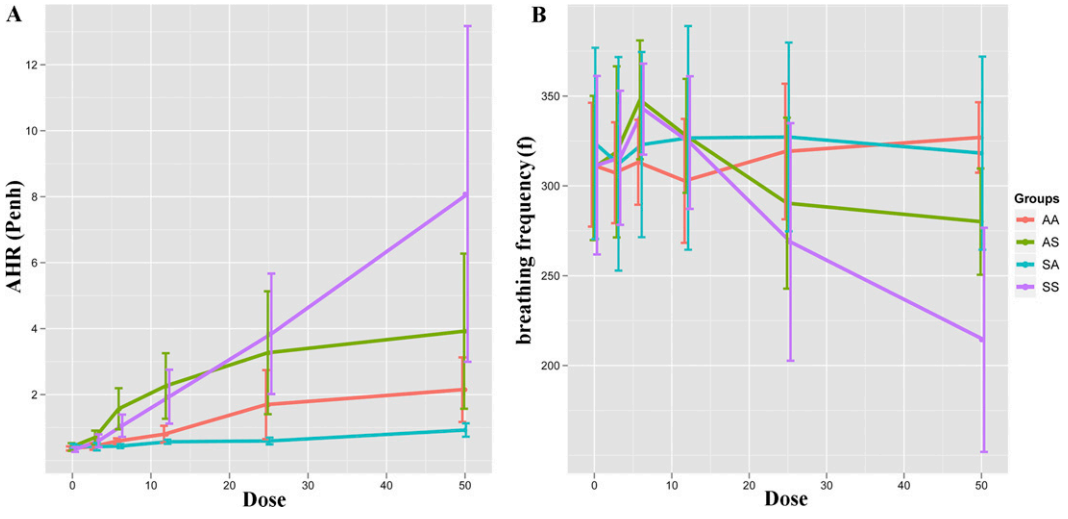

Figure 4. Whole-body plethysmography showed significantly increased airway hyperresponsiveness (AHR) (Penh) and decreased breathing frequency (f) in mice twice-exposed to SHS, compared with those exposed either only *in utero* or as adults. Significant differences (ANOVA, $P < 0.05$) were found in Penh (all methacholine doses) and f (only 50 mg/ml). The *post hoc* Tukey honest significant difference test indicates that differences existed between SS and at least one other group at methacholine concentrations < 6 mg/ml and between SS and all other groups when treated with methacholine at 50 mg/ml. Values are represented as mean ± SD.

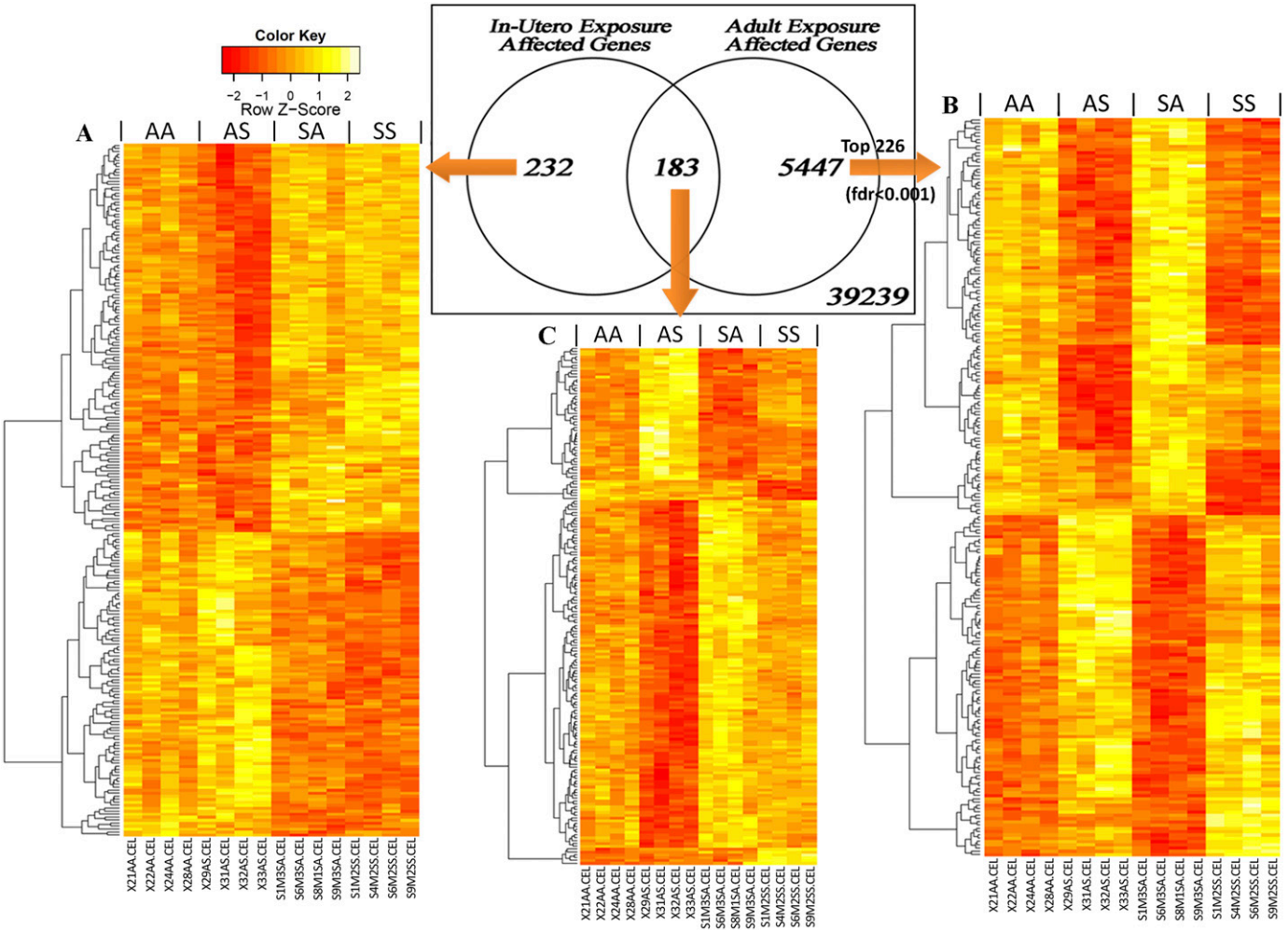

Figure 5. Transcriptome screening in lungs of 15-week-old male mice revealed subsets of genes that are associated predominantly with (*A*) *in utero* exposure, (*B*) adult exposure, and (C) mixed effects of both. The Venn diagram shows numbers of probes found to be significantly expressed during each exposure period (false discovery rate [FDR] < 0.05). Heat maps show the expression pattern of probes in each portion of the Venn diagram. For the adult exposure effect ($>$ 5,000 probes), 226 gene probes with FDR < 0.001 are presented.

set at zero. An absolute difference of 1 in the units on the *y* axis indicates a 2-fold difference in expression.

We found a minimum fold-change of two for all the genes charted in Figure 7B, including *in utero* exposure–affected genes (Egr1 and Fos), both (*in utero* and adult) exposure-affected genes (Btg2, Zfp36, and Nr4a1), and AHR-associated genes (Gata3, Fam107a, Cyp1a1, and Adamts9). The high correlation between AHR responses and SS exposures is reflected in the relative expression levels of Fam107, Cyp1a1, and Adamts9.

In utero SHS exposure identified genes primarily associated with immune system processes (GO, 0002376; $P = 1.18E\text{-}8$; FDR = 5.92E-6), most of which are not responsive to adult SHS exposure. The most striking KEGG pathways of adult exposure–affected genes included "circadian rhythm, mammal" ($P = 2.59E\text{-}07$; FDR = 4.40E-05), "mitogen-activated protein kinase signaling pathway" ($P = 0.0005$; FDR = 0.0340), and "pathways in cancer" ($P = 0.0006$; FDR = 0.0340) (online supplement).

We further combined the *in utero* exposure–affected gene-list with the AHR-associated gene list and searched for distinct signaling pathways from the newly generated gene list in IPA. The enriched canonical pathways found included "IL-17A signaling in fibroblasts" ($P = 2.24E\text{-}4$) and "production of nitric oxide and reactive oxygen species in macrophages" ($P = 2.09E\text{-}3$). By connecting genes with reported gene interactions and known biological function, a composite gene network was built, as depicted in Figure 7C. The additional two IPA-designated biological functions shown in Figure 7C are "inflammation" ($P = 1.02E\text{-}8$) and "hypersensitive reaction" ($P = 1.1E\text{-}8$). Genes associated with the IL-17A signaling pathway, including Cebpd, Nfkbia, Ccl2, and Fos, also appear in the inflammation and reactive oxygen species pathways (Figure 7C).

DISCUSSION

The experiments described here demonstrate that *in utero* exposure to environmentally relevant concentrations of SHS modulates adult responses to subsequent SHS exposures. Male BALB/c mice exposed to SHS both *in utero* and as adults exhibited significantly elevated lung morphometry, pulmonary function, and gene expression responses, compared with the other three groups. Somewhat surprisingly, none of these changes appeared to be driven by inflammatory processes. Although concentrations of the proinflammatory cytokines IL-1b, IL-6, and KC were significantly elevated in the BAL fluid of SS mice, the concentrations of each (IL-1b = 2.7 pg/ml, IL-6 = 7.9 pg/ml, and KC = 49.5 pg/ml; Figure 2) were near the low end of their respective linear response ranges, which at their high end range from 10,000–100,000 pg/ml. Although the

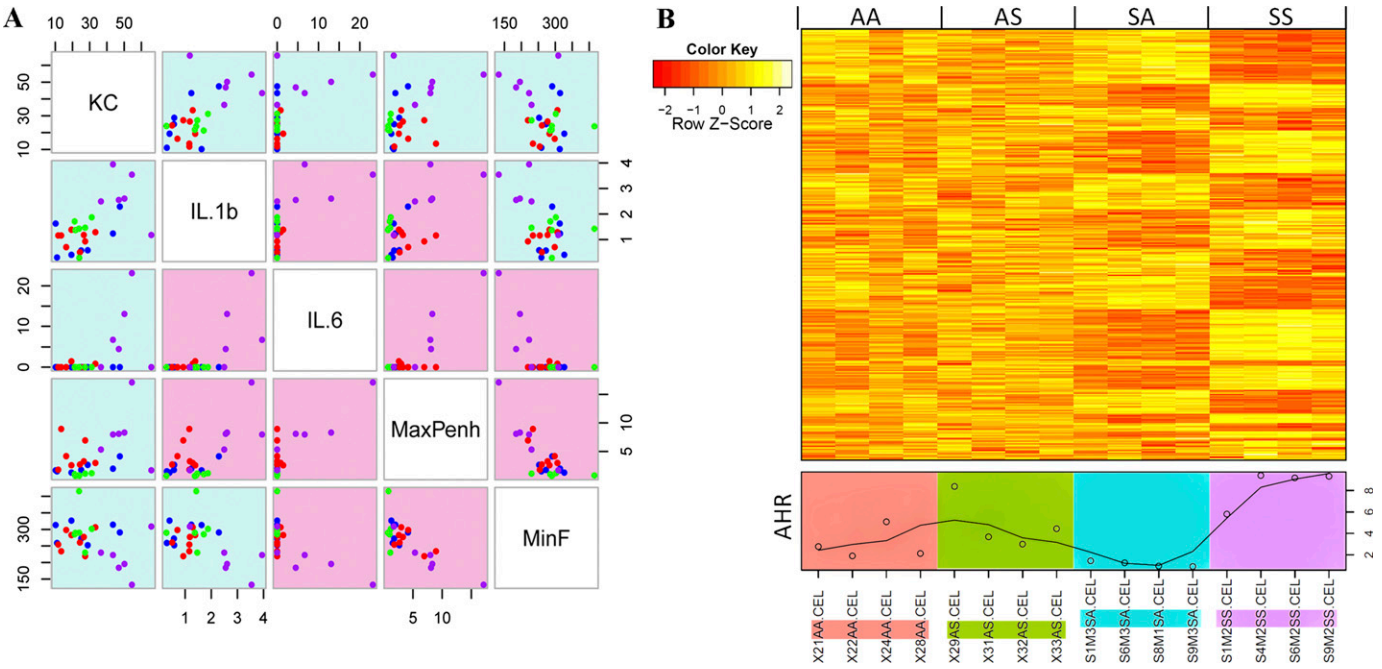

Figure 6. Physiological and cytokine measurements were highly correlated, and can be associated with subsets of genes through microarray analysis. (*A*) All readings are reported in the same units as in other figures, e.g., pg/ml for cytokines, plotted to interrogate the correlation between every two parameters (color of each dot, AA = *blue*, AS = *red*, SA = *green*, and SS = *purple*). All measurements demonstrated a fairly high correlation with each other ($|r| > 0.5$). The background color of each scatterplot indicates the degree of correlation (*blue* = moderate, and *red* = high). (*B*) Three hundred and twenty-three gene probes, significantly correlated with AHR (represented by MaxPenh values), are shown in a heat map with each animal's MaxPenh values plotted below (*actual dots with a smoothed line*). The correlation graph was plotted with the GCLUS package in R/bioconductor (see MATERIALS AND METHODS). Max, maximum; Min, minimum.

absence of IFN-γ and IL-12 from all groups is consistent with previous reports of a blunted Th1 response in murine lungs exposed to SHS (23, 24), their absence may equally well reflect an overall weak cytokine response to SHS exposures. The absence of grossly visible inflammation or increased immune cell infiltration in all four groups is consistent with this weak cytokine response.

Morphometric analysis provided quantitative values for the evaluation of lung structural changes in response to SHS exposures. The lack of significant statistical differences between the four groups before pooling likely reflects the relatively low numbers in each group (6–8). Further statistical analysis identified significant differences after regrouping mice into two groups, according to their *in utero* exposure status. Mice exposed *in utero* to SHS (SA and SS) demonstrated higher MLI values than those exposed to AIR *in utero* (AA and AS). This finding suggests airspace enlargement in mice exposed *in utero* to SHS. In addition, the wall thickness and external diameter of random selected medium-sized arteries were significantly increased in animals exposed *in utero* to SHS. Together, these data indicate a role for *in utero* exposure to SHS in lung development that is sustained into adulthood. In this case, the effects of 2 weeks of *in utero* exposure (SA and SS) outweighed the effects of 4 weeks of adult SHS (AS).

Increased collagen deposition around the lung arteries in the AS and SS groups (Figure 3B) suggests that adult exposure results in the production of more extracellular matrix (ECM) proteins, which would ultimately be necessary for the development of lung fibrosis and COPD. The pathogenesis of COPD is associated with an imbalance of metalloproteases (matrix metalloproteases [MMP] and a disintegrin and metalloprotease) and antimetalloproteases (tissue inhibitor of metalloproteases and α-2M) (25). In the present study, a notable up-regulation of metalloprotease family genes was evident, including Adamts9 and Mmp3 in the SS and AHR groups (a 2–4 times increase). The up-regulation of both of these genes has been associated with lung fibrosis. Adamts9 up-regulation and associated collagen deposition have been reported in a TGF-β–stimulated model of lung fibrosis (26). The collagen deposition was reduced in alveolar epithelial cells transfected with Adamts9 small interfering (si)RNA. Paraquat-induced lung fibrosis in mice also is associated with Mmp3 up-regulation (27). In addition to lung structural changes, *in utero* SHS exposure may exert an effect on the pathogenesis of COPD. An epidemiological study in 2009 linked maternal smoke exposure to further impaired lung function in offspring even in late adulthood, when COPD becomes apparent. Furthermore, maternal smoke exposure aggravated the cumulative effect of active cigarette consumption (28). Together, these results suggest that early-life exposure to smoke may serve as a risk factor for the pathogenesis of COPD.

Lung function testing revealed that the SS group was more responsive than the other three groups at the highest methacholine dose (50 mg/ml) in terms of both Penh and breathing frequency. Although Penh does not directly reflect airway mechanical function (29), it has been used as an indicator of AHR, and was shown to correlate well with lung resistance in BALB/c mice (30, 31). Together with the observed reduction in breathing frequency, likely an adaptive response to bronchoconstriction (32), these results strongly support a significantly enhanced airway response in the group that was exposed to SHS both *in utero* and as adults. An earlier report described similar results in rats exposed *in utero* and then postnatally to SHS. Significantly increased lung resistance was evident, compared with SHS exposure at one timepoint only, at 7–10 weeks of age (33).

Gene expression profiling with a linear model revealed that the most differentially expressed genes associated with *in utero* SHS exposure include Fos, Egr1, and Cyr61, all of which are down-regulated > 2 times. These results were confirmed by

A

In utero exposure affected genes		Both exposure affected genes		Adult exposure affected genes		AHR associated genes	
Up	Down	Up	Down	Up	Down	Up	Down
NTRK2 1.685	FOS -3.154	CYP1A1 2.759	PRR5L -1.560	ZBTB16* 5.391	LRAT* -2.044	ADAMTS9 3.379	CASS4 -2.156
SALL1 1.516	EGR1 -2.916	ERRFI1 1.631	JUNB -1.528	APOLD1 3.646	CCR2* -2.020	CYP1A1 2.759	CXCR4 -1.789
SHROOM2 1.413	CYR61* -2.040	CALCB 1.525	TRIM14 -1.489	FKBP5* 3.449	Iigp1/Iigp1b* -1.901	SORBS1* 2.337	HHEX -1.725
PELI2 1.341	FCER2 -1.944	PER1 1.506	IER2 -1.411	ADAMTS9* 3.379	ELK3* -1.876	MPP3 2.311	PRDM8 -1.715
Glt28d2 1.327	PDE4B -1.900	RASD1 1.431	FOXP1 -1.409	CYP1A1 2.759	IGKC* -1.873	FAM107A* 2.219	GATA3 -1.708
CAMTA1 1.325	CFD -1.774	CSRNP1 1.408	LCP2 -1.332	CDKN1A* 2.509	PTPRC -1.854	UCP2 2.192	Ifi47 -1.690
RGS7BP 1.314	FOSB -1.772	ZHX3 1.378	NR4A1 -1.329	SORBS1* 2.337	MEIS2 -1.821	MAP3K6 2.095	MYCT1 -1.685
PDLIM5 1.302	CCL2 -1.763	FRY 1.362	ZFP36 -1.326	MPP3* 2.311	GPR34 -1.820	Retnla 2.037	PCDH17* -1.670
TTLL7* 1.291	LTB -1.762	BCAR3 1.293	BTG2 -1.297	CREB5* 2.235	CXCR4 -1.789	LMCD1 1.969	SOX4* -1.659
HECW2 1.287	CD79A -1.733	ADRB2 1.281	DUSP1 -1.224	FAM107A* 2.219	NPPA -1.764	CCRN4L 1.963	ANKMY2* -1.633

B

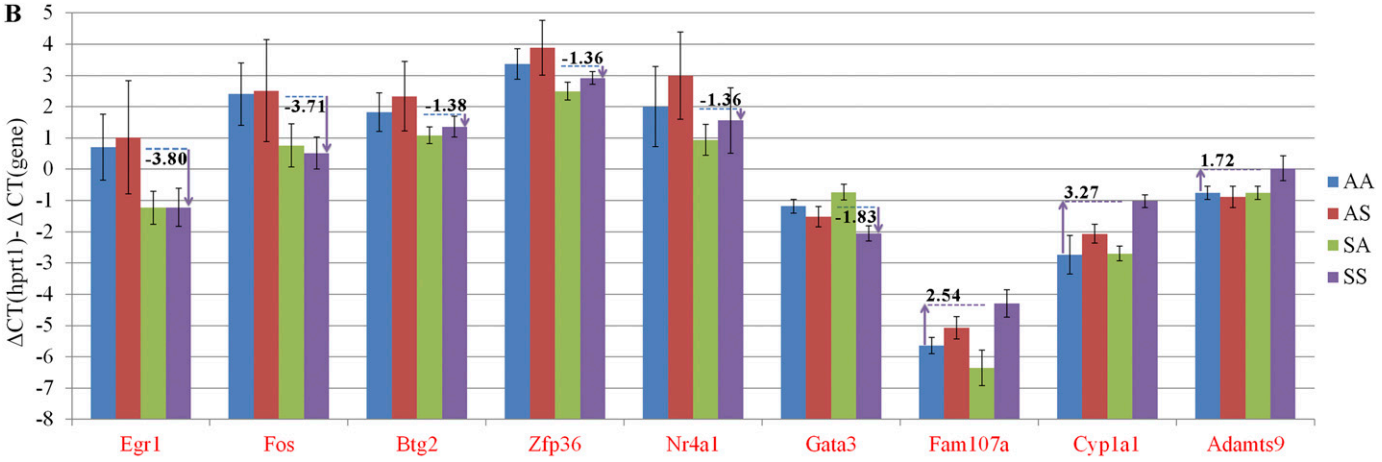

C

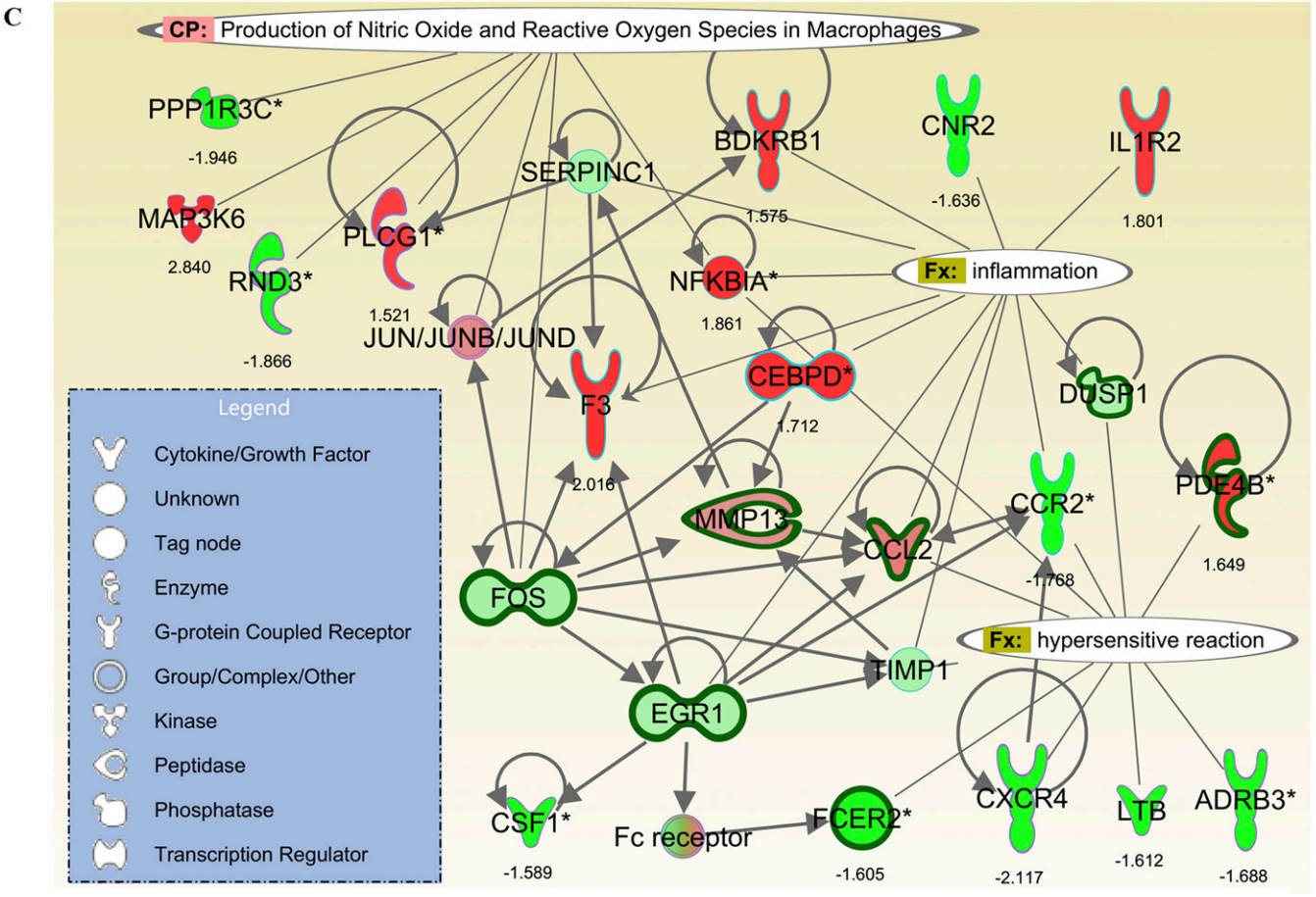

quantitative RT-PCR (Figure 7B). In adults, the up-regulation of these three genes has been associated with COPD progression (34). Egr1, a zinc finger transcription factor, was suggested to play a key role in the development of cigarette smoke–induced COPD by regulating MMP activity, and then affecting the turnover of ECM proteins during the pathogenesis of COPD (35). Fos is an important component of activator protein–1 (AP-1), a redox-sensitive transcription factor, which interacts with Nrf2 (nuclear factor erythroid–derived 2, like 2) and regulates cytoprotective enzymes, including heme oxygenase (36). Reductions in

Figure 7. (*A*) Microarray fold-changes between SS and AA (doubly exposed to SHS versus never exposed) are listed for the 10 most up-regulated/down-regulated genes in each of the four gene sets (*in utero*, adult, both, and AHR). Genes highlighted in *red* were confirmed by quantitative RT-PCR. (*B*) Quantitative RT-PCR, performed on nine genes, yielded comparable fold-change values (numbers shown for each gene) between SS (*purple*) and AA (*blue*), which confirmed the microarray-based findings. Data (*y* axis) are presented as differences in threshold cycle ($-\Delta\Delta$CT) values, so that calculated values are positively associated with gene expression levels. For each comparison, the Hprt1 value is set at zero. (*C*) Genes affected by *in utero* exposure and those highly correlated with AHR were interconnected in IPA Pathway Designer, and were found to be significantly associated with several known biological functions and canonical pathways ($P < 0.05$). *Thickened dark green edges* indicate significant down-regulation attributable to *in utero* SHS exposure (SX versus AX); colors inside each node indicate gene expression changes with increased AHR (SS versus SA, *red*/*green* = up-regulation/down-regulation).

Fos expression induced by cigarette smoke may interfere with protection against oxidative stress. Two other genes with approximately 2-fold down-regulation after *in utero* SHS exposure are Fcer2 and Pde4b, both of which have single-nucleotide proteins linked to increased risks of asthma and COPD. Fcer2 (the Fc fragment of IgE, a low-affinity II receptor) encodes the low-affinity IgE receptor, CD23, which is a key regulator in the biologic actions of IgE-mediated hypersensitivity commonly found in patients with asthma (37). Pde4b, which encodes the cyclic adenosine monophosphate–specific 3′,5′-cyclic phosphodiesterase 4B, has been identified as an essential molecule for Th2 cell function and the development of AHR in allergic asthma (38).

The decreased expression here of Fos, Egr1, and Cyr61 in mice exposed *in utero* to SHS contrasts with clinical and experimental findings from adult mainstream smoke exposures, as already noted, that have linked the elevated expression of these genes with the progression of asthma or COPD. Clearly, the suppressed expression of these genes associated with *in utero* SHS exposure did not protect against indicators of these diseases here, because more airspaces were found in the SA and SS groups and significantly increased AHR was observed in the SS group. In addition, the up-regulation of the profibrotic Adamts9 and Mmp3 in the lungs of SS-exposed adult mice is also consistent with a COPD-promoting effect. The possibility of a relationship between gestational SHS exposure and the subsequent development of COPD has apparently not been previously examined. Alternatively, the unexpected down-regulation of Fos, Egr1, and Cyr61, despite the accompanying increases in airspaces, collagen deposition, and AHR in the lungs of adult mice exposed *in utero* to SHS, may simply be consistent with the view that no good animal models of cigarette smoke–associated COPD have been established (39).

Although the approach we adopted successfully selected candidate genes according to how closely they matched smoke exposure conditions, the gene expression results we observed relating to whole-body plethysmography and cytokine responses were markedly enhanced only in animals exposed to SHS both *in utero* and as adults (Figure 6). To identify the genes closely correlated with the prominent SS response, the most prominent of the functional lung responses, MaxPenh, was selected as the response variable to which gene expression changes were compared. Among the merits of this approach, gene-response correlation values were calculated regardless of the group in which each sample resided, so that the in-group variation will not negatively affect the test results. This is illustrated in the sample labeled "29AS," where the high AHR response in an otherwise low AHR group was correlated with levels of gene expression comparable to those found in all four mice in the high AHR SS group (Figure 6B).

To investigate further how *in utero* SHS exposure may contribute to exacerbated adult responses, we combined the lists of *in utero* only exposure–affected genes with AHR-associated genes, and interrogated signaling pathways from this new gene list. From IPA, the AHR-associated genes were recognized to be significantly associated with increased inflammation, oxidative stress, and hypersensitivity reactions. Although the fold-change values (SS versus SA, and highest versus lowest AHR; see Figures 4A and 6B) in the gene network (Figure 7C) were moderate ($\times$1.5–$\times$2.8), they were all observed in genes modulated by *in utero* SHS exposure, and were retained until 15 weeks of age.

In addition, IL-17 signaling, one of the most significant canonical pathways identified in IPA with *in utero* exposure (P = 6.12E-03), as well as with both exposures (P = 2.05E-03), may also partly explain the prominent SS response that originates from *in utero* SHS exposures. Because fetal T cells develop during the second trimester of gestation (40), the changes in cytokine concentrations are detected not only in the circulating blood of the pregnant mothers, but also in amniotic fluids in direct contact with the fetal lungs (41). The elevated circulating concentration of TGF-β during gestation promotes the development of regulatory T cells. However, *in utero* SHS exposure also increases the concentrations of IL-6, and naive T cells will differentiate into Th17 cells in the presence of both TGF-β and IL-6 (42). In addition, the aryl hydrocarbon receptor, which is activated by the polynuclear aromatic hydrocarbons generated by cigarette smoke, was also reported to exhibit regulatory functions in Th17 cell populations (43–45). During the critical developmental period, the immune cell lineage commitment may greatly affect the lung responses of offspring, even when they become adults (46).

In conclusion, we examined the lung responses of BALB/c mice to *in utero* and adult exposures to environmentally relevant concentrations of SHS. Significant increases occurred in AHR and in proinflammatory cytokine production (IL-1b, IL-6, and KC), albeit at low concentrations, in lungs of 15-week-old doubly exposed mice. Enlarged airspaces and arteries were evident in the lungs of mice exposed *in utero* to SHS, in addition to increased collagen deposition around those arteries in mice exposed to SHS as adults. Unique gene expression patterns were apparent for *in utero*, adult, and combined exposures. Overall, the results indicate that *in utero* SHS exposures alter lung structure more severely than do adult SHS exposures of longer duration. In addition, *in utero* SHS exposures aggravate AHR and promote a profibrotic milieu in adult lungs.

Author disclosures are available with the text of this article at www.atsjournals.org.

Acknowledgments: The authors thank Lindsey Clemones of the Louisiana State University School of Veterinary Medicine and Paula Polk of the Research Core Facility of the Louisiana State University Health Science Center at Shreveport for excellent technical assistance.

References

1. Lindfors A, van Hage-Hamsten M, Rietz H, Wickman M, Nordvall SL. Influence of interaction of environmental risk factors and sensitization in young asthmatic children. *J Allergy Clin Immunol* 1999;104:755–762.
2. Mannino DM, Moorman JE, Kingsley B, Rose D, Repace J. Health effects related to environmental tobacco smoke exposure in children in the United States: data from the Third National Health and Nutrition Examination Survey. *Arch Pediatr Adolesc Med* 2001;155:36–41.
3. Gilliland FD, Berhane K, McConnell R, Gauderman WJ, Vora H, Rappaport EB, Avol E, Peters JM. Maternal smoking during pregnancy, environmental tobacco smoke exposure and childhood lung function. *Thorax* 2000;55:271–276.
4. Gilliland FD, Li YF, Peters JM. Effects of maternal smoking during pregnancy and environmental tobacco smoke on asthma and wheezing in children. *Am J Respir Crit Care Med* 2001;163:429–436.

5. Gilliland FD, Berhane K, Li YF, Rappaport EB, Peters JM. Effects of early onset asthma and *in utero* exposure to maternal smoking on childhood lung function. *Am J Respir Crit Care Med* 2003;167:917–924.
6. Li YF, Gilliland FD, Berhane K, McConnell R, Gauderman WJ, Rappaport EB, Peters JM. Effects of *in utero* and environmental tobacco smoke exposure on lung function in boys and girls with and without asthma. *Am J Respir Crit Care Med* 2000;162:2097–2104.
7. Zlotkowska R, Zejda JE. Fetal and postnatal exposure to tobacco smoke and respiratory health in children. *Eur J Epidemiol* 2005;20:719–727.
8. Penn AL, Rouse RL, Horohov DW, Kearney MT, Paulsen DB, Lomax L. *In utero* exposure to environmental tobacco smoke potentiates adult responses to allergen in BALB/c mice. *Environ Health Perspect* 2007;115:548–555.
9. Rouse RL, Boudreaux MJ, Penn AL. *In utero* environmental tobacco smoke exposure alters gene expression in lungs of adult Balb/c mice. *Environ Health Perspect* 2007;115:1757–1766.
10. Raherison C, Penard-Morand C, Moreau D, Caillaud D, Charpin D, Kopferschmitt C, Lavaud F, Taytard A, Maesano IA. Smoking exposure and allergic sensitization in children according to maternal allergies. *Ann Allergy Asthma Immunol* 2008;100:351–357.
11. Singh SP, Gundavarapu S, Pena-Philippides JC, Rir-Sima-ah J, Mishra NC, Wilder JA, Langley RJ, Smith KR, Sopori ML. Prenatal secondhand cigarette smoke promotes Th2 polarization and impairs goblet cell differentiation and airway mucus formation. *J Immunol* 2011;187:4542–4552.
12. Kajekar R. Environmental factors and developmental outcomes in the lung. *Pharmacol Ther* 2007;114:129–145.
13. Sethi JM, Rochester CL. Smoking and chronic obstructive pulmonary disease. *Clin Chest Med* 2000;21:67–86. (viii.).
14. Bowles K, Horohov D, Paulsen D, Leblanc C, Littlefield-Chabaud M, Ahlert T, Ahlert K, Pourciau S, Penn A. Exposure of adult mice to environmental tobacco smoke fails to enhance the immune response to inhaled antigen. *Inhal Toxicol* 2005;17:43–51.
15. Penn A, Snyder CA. Inhalation of sidestream cigarette smoke accelerates development of arteriosclerotic plaques. *Circulation* 1993;88:1820–1825.
16. Altria Client Services, Inc. Comments on draft guidance entitled "Reporting Harmful and Potentially Harmful Constituents in Tobacco Products and Tobacco Smoke under the Federal Food, Drug, and Cosmetic Act." Available from: http://www.Altria.Com/en/cms/about_altria/federal-regulation-of-tobacco/regulatory-filings/pdfs/reporting-harmful-and-potentially-harmful-constituents.Pdf.Aspx?Src=search&q=reporting-harmful-and-potentially-harmful-constituents.Pdf. 2012.
17. Penn A, Chen LC, Snyder CA. Inhalation of steady-state sidestream smoke from one cigarette promotes arteriosclerotic plaque development. *Circulation* 1994;90:1363–1367.
18. Ambalavanan N, Nicola T, Hagood J, Bulger A, Serra R, Murphy-Ullrich J, Oparil S, Chen YF. Transforming growth factor–beta signaling mediates hypoxia-induced pulmonary arterial remodeling and inhibition of alveolar development in newborn mouse lung. *Am J Physiol Lung Cell Mol Physiol* 2008;295:L86–L95.
19. Smyth GK. Linear models and empirical Bayes methods for assessing differential expression in microarray experiments. *Stat Appl Genet Mol Biol* 2004;3:Article3.
20. Planet E. Phenotest: tools to test association between gene expression and phenotype in a way that is efficient, structured, fast and scalable (accessed 17 May 2011). Available from: http://bioconductor.org/packages/2.11/bioc/html/phenoTest.html.
21. Ploner A. Heatplus: heatmaps with row and/or column covariates and colored clusters (accessed 18 May 2011). Available from: http://bioconductor.org/packages/2.11/bioc/html/Heatplus.html.
22. Duncan DT, Prodduturi N, Zhang B. Webgestalt2: an updated and expanded version of the web-based gene set analysis toolkit. *BMC Bioinformatics* 2010;11:10.
23. Adkins B, Bu Y, Guevara P. The generation of Th memory in neonates versus adults: prolonged primary Th2 effector function and impaired development of Th1 memory effector function in murine neonates. *J Immunol* 2001;166:918–925.
24. Phaybouth V, Wang SZ, Hutt JA, McDonald JD, Harrod KS, Barrett EG. Cigarette smoke suppresses Th1 cytokine production and increases RSV expression in a neonatal model. *Am J Physiol Lung Cell Mol Physiol* 2006;290:L222–L231.
25. Mocchegiani E, Giacconi R, Costarelli L. Metalloproteases/antimetalloproteases imbalance in chronic obstructive pulmonary disease: genetic factors and treatment implications. *Curr Opin Pulm Med* 2011;17:S11–S19.
26. Keating DT, Sadlier DM, Patricelli A, Smith SM, Walls D, Egan JJ, Doran PP. Microarray identifies ADAM family members as key responders to TGF-beta1 in alveolar epithelial cells. *Respir Res* 2006;7:114.
27. Tomita M, Okuyama T, Katsuyama H, Miura Y, Nishimura Y, Hidaka K, Otsuki T, Ishikawa T. Mouse model of paraquat-poisoned lungs and its gene expression profile. *Toxicology* 2007;231:200–209.
28. Beyer D, Mitfessel H, Gillissen A. Maternal smoking promotes chronic obstructive lung disease in the offspring as adults. *Eur J Med Res* 2009;14:27–31.
29. Hamelmann E, Schwarze J, Takeda K, Oshiba A, Larsen GL, Irvin CG, Gelfand EW. Noninvasive measurement of airway responsiveness in allergic mice using barometric plethysmography. *Am J Respir Crit Care Med* 1997;156:766–775.
30. DeLorme MP, Moss OR. Pulmonary function assessment by whole-body plethysmography in restrained versus unrestrained mice. *J Pharmacol Toxicol Methods* 2002;47:1–10.
31. Singh SP, Barrett EG, Kalra R, Razani-Boroujerdi S, Langley RJ, Kurup V, Tesfaigzi Y, Sopori ML. Prenatal cigarette smoke decreases lung cAMP and increases airway hyperresponsiveness. *Am J Respir Crit Care Med* 2003;168:342–347.
32. Adler A, Cieslewicz G, Irvin CG. Unrestrained plethysmography is an unreliable measure of airway responsiveness in BALB/c and C57BL/6 mice. *J Appl Physiol* 2004;97:286–292.
33. Joad JP, Ji C, Kott KS, Bric JM, Pinkerton KE. *In utero* and postnatal effects of sidestream cigarette smoke exposure on lung function, hyperresponsiveness, and neuroendocrine cells in rats. *Toxicol Appl Pharmacol* 1995;132:63–71.
34. Ning W, Li CJ, Kaminski N, Feghali-Bostwick CA, Alber SM, Di YP, Otterbein SL, Song R, Hayashi S, Zhou Z, *et al*. Comprehensive gene expression profiles reveal pathways related to the pathogenesis of chronic obstructive pulmonary disease. *Proc Natl Acad Sci USA* 2004;101:14895–14900.
35. Reynolds PR, Cosio MG, Hoidal JR. Cigarette smoke–induced Egr-1 upregulates proinflammatory cytokines in pulmonary epithelial cells. *Am J Respir Cell Mol Biol* 2006;35:314–319.
36. Baglole CJ, Sime PJ, Phipps RP. Cigarette smoke–induced expression of heme oxygenase–1 in human lung fibroblasts is regulated by intracellular glutathione. *Am J Physiol Lung Cell Mol Physiol* 2008;295:L624–L636.
37. Tantisira KG, Silverman ES, Mariani TJ, Xu J, Richter BG, Klanderman BJ, Litonjua AA, Lazarus R, Rosenwasser LJ, Fuhlbrigge AL, *et al*. FCER2: a pharmacogenetic basis for severe exacerbations in children with asthma. *J Allergy Clin Immunol* 2007;120:1285–1291.
38. Jin SL, Goya S, Nakae S, Wang D, Bruss M, Hou C, Umetsu D, Conti M. Phosphodiesterase 4B is essential for T(H)2-cell function and development of airway hyperresponsiveness in allergic asthma. *J Allergy Clin Immunol* 2010;126:1252–1259.
39. Churg A, Sin DD, Wright JL. Everything prevents emphysema: are animal models of cigarette smoke–induced chronic obstructive pulmonary disease any use? *Am J Respir Cell Mol Biol* 2011;45:1111–1115.
40. Papiernik M. Correlation of lymphocyte transformation and morphology in the human fetal thymus. *Blood* 1970;36:470–479.
41. Mandal M, Marzouk AC, Donnelly R, Ponzio NM. Maternal immune stimulation during pregnancy affects adaptive immunity in offspring to promote development of Th17 cells. *Brain Behav Immun* 2011;25:863–871.
42. Bettelli E, Carrier Y, Gao W, Korn T, Strom TB, Oukka M, Weiner HL, Kuchroo VK. Reciprocal developmental pathways for the generation of pathogenic effector Th17 and regulatory T cells. *Nature* 2006;441:235–238.
43. Quintana FJ, Basso AS, Iglesias AH, Korn T, Farez MF, Bettelli E, Caccamo M, Oukka M, Weiner HL. Control of T(reg) and T(H)17 cell differentiation by the aryl hydrocarbon receptor. *Nature* 2008;453:65–71.
44. Veldhoen M, Hirota K, Westendorf AM, Buer J, Dumoutier L, Renauld JC, Stockinger B. The aryl hydrocarbon receptor links Th17-cell–mediated autoimmunity to environmental toxins. *Nature* 2008;453:106–109.
45. Kimura A, Naka T, Nohara K, Fujii-Kuriyama Y, Kishimoto T. Aryl hydrocarbon receptor regulates Stat1 activation and participates in the development of Th17 cells. *Proc Natl Acad Sci USA* 2008;105:9721–9726.
46. Martino DJ, Prescott SL. Silent mysteries: epigenetic paradigms could hold the key to conquering the epidemic of allergy and immune disease. *Allergy* 2010;65:7–15.